

BCSJ Award Article

Photocatalytic Electron-Transfer Oxidation of Triphenylphosphine and Benzylamine with Molecular Oxygen via Formation of Radical Cations and Superoxide Ion

Kei Ohkubo, Takashi Nanjo, and Shunichi Fukuzumi*

Department of Material and Life Science, Graduate School of Engineering, Osaka University, Suita, Osaka 565-0871

SORST, Japan Science and Technology Agency (JST), Suita, Osaka 565-0871

Received April 20, 2006; E-mail: fukuzumi@chem.eng.osaka-u.ac.jp

Photooxygenation of triphenylphosphine (Ph_3P) to triphenylphosphine oxide ($Ph_3P{=}O$) with molecular oxygen (O_2) occurs under photoirradiation of 9-mesityl-10-methylacridinium perchlorate ($[Acr^+–Mes]ClO_4^-$) which acts as an efficient electron-transfer photocatalyst. Photooxidation of benzylamine ($PhCH_2NH_2$) with O_2 also occurs efficiently under photoirradiation of Acr^+–Mes to yield $PhCH_2N{=}CHPh$ and hydrogen peroxide (H_2O_2). Each photocatalytic reaction is initiated by intramolecular photoinduced electron transfer from the Mes moiety to the singlet excited state of the Acr^+ moiety to produce the electron-transfer state ($Acr^•–Mes^{•+}$). The $Mes^{•+}$ moiety oxidizes Ph_3P and $PhCH_2NH_2$ to produce the radical cations ($Ph_3P^{•+}$ and $PhCH_2NH_2^{•+}$, respectively), whereas the $Acr^•$ moiety reduces O_2 to $O_2^{•-}$. The produced $Ph_3P^{•+}$ binds with $O_2^{•-}$ as well as O_2, leading to the oxygenated product ($Ph_3P{=}O$). On the other hand, proton transfer from $PhCH_2NH_2^{•+}$ to $O_2^{•-}$ occurs, followed by hydrogen transfer, leading to the dehydrogenated dimer product, $PhCH_2N{=}CHPh$. In each case, the radical intermediates were detected by laser flash photolysis and ESR measurements to clarify the photocatalytic mechanism.

Free radicals are highly versatile and reactive intermediates, allowing many syntheses to be carried out under relatively mild conditions in chemical and biological systems.[1–4] However, the high reactivity of free radicals usually results in low selectivity and thus, it has been difficult to utilize reactions between free radicals for selective bond formation.[1–4] In contrast to neutral free radicals, reactions of radical ions are well controlled by charges because radical cations are expected to react selectively with radical anions as compared with reactions of radical ions with the same charge. Thus, reactions between radical cations and radical anions have profound fundamental and synthetic interest for selective bond formation.[5–11]

Radical cations and radical anions can be produced photochemically by electron transfer from photoexcited electron donors (D^*: * denotes the photoexcited state) to electron acceptors (A) or from electron donors (D) to photoexcited electron acceptors (A^*).[12–17] Radical ion pairs can also be produced by photoexcitation of the charge-transfer complex between D and A.[18–26] However, reactions between $D^{•+}$ and $A^{•-}$ often result in back electron transfer from $A^{•-}$ to $D^{•+}$ to reproduce the reactant pair (D and A) without the formation of a chemical bond. This back electron transfer from $A^{•-}$ to $D^{•+}$ can be retarded by choosing an appropriate substance, which has large reorganization energy for electron transfer. Molecular oxygen (O_2) is suitable for such a purpose, because electron-transfer reactions of O_2 are known to be rather slow because of the large reorganization energy of electron transfer.[27–31] In the case of O_2, however, the excited state (singlet oxygen) is frequently formed in reactions involving photoexcited states via energy transfer, reacting directly with substrates.[32–35] Thus, it is highly desired to avoid such an energy-transfer process for the selective reaction between radical cations and $O_2^{•-}$.

We have recently reported that the photoexcitation of 9-mesityl-10-methylacridinium ion (Acr^+–Mes) results in ultrafast electron transfer from the Mes moiety to the singlet excited state of the Acr^+ moiety to form the electron-transfer state ($Acr^•–Mes^{•+}$), which has an extremely long lifetime (e.g., 2 h at 203 K) and a high energy (2.37 eV).[36,37] The electron-transfer state ($Acr^•–Mes^{•+}$) is both a strong oxidizing agent with the $Mes^{•+}$ moiety and the a strong reducing agent with the $Acr^•$ moiety.[36,37] In such a case, Acr^+–Mes acts as an efficient electron-transfer photocatalyst for highly selective oxygenation of anthracene and tetraphenylethylene with O_2 via selective radical coupling of the donor radical cations and $O_2^{•-}$ under visible light irradiation to produce epidioxyanthracene and 1,2-dioxetane, respectively.[38,39] However, the use of Acr^+–Mes as an efficient electron-transfer photocatalyst has yet to be expanded to photooxidation of substrates with O_2 other than cycloadditions.

Herein, we expand the scope of the use of Acr^+–Mes as an

Published on the web October 10, 2006; doi:10.1246/bcsj.79.1489

efficient electron-transfer photocatalyst for oxidation of organic compounds with O_2 other than oxygenation reactions by examining photocatalytic oxidation of triphenylphosphine and benzylamine with O_2 in the presence of Acr^+–Mes. The photocatalytic mechanisms are clarified by detecting radical intermediates involved in the photocatalytic reactions with use of laser flash photolysis and ESR measurements.

Experimental

Materials. Benzylamine, *N*,*N*-dimethylbenzylamine, *N*-benzylidenebenzylamine, and triphenylphosphine oxide ($Ph_3P{=}O$) were obtained from Tokyo Kasei Kogyo Co., Ltd. Triphenylphosphine (Ph_3P) was obtained from Sigma-Aldrich Co., Ltd. Di-*t*-butylperoxide (Bu^tOOBu^t) was obtained from Nakalai Tesque Co., Ltd. Acetonitrile (MeCN) and chloroform ($CHCl_3$) were of spectral grade, obtained commercially and used without further purification.

9-Mesityl-10-methylacridinium perchlorate ($[Acr^+–Mes]ClO_4^-$) was prepared by the reaction of 10-methylacridone with mesityl magnesium bromide (MesMgBr) in tetrahydrofuran, followed by addition of sodium hydroxide (water) for hydrolysis and perchloric acid for neutralization.[38] The compound was purified by recrystallization from methanol–diethyl ether. The yield was 87% based on acridone.[40] ^1H NMR (CD_3CN, 300 MHz) δ (ppm) 8.16 (d, $J = 9.0$ Hz, 2H), 7.93 (t, $J = 9.0$ Hz, 2H), 7.40 (s, 4H), 6.79 (s, 2H), 4.37 (s, 3H), 2.02 (s, 3H), 1.25 (s, 6H). Anal. Calcd for $C_{23}H_{22}ClNO_4$: C, 67.07; H, 5.38; N, 3.40%. Found: C, 66.78; H, 5.33; N, 3.35%. 10-Methylacridinium iodide ($AcrH^+I^-$) was prepared by the reaction of acridine with methyl iodide in acetone and was converted to the perchlorate salt ($AcrH^+ClO_4^-$) by the addition of magnesium perchlorate to the iodide salt ($AcrH^+I^-$), and purified by recrystallization from methanol.[41] Synthesis of [*N*,*N*-$^2H_2$]benzylamine was carried out according to the literature.[42] A solution containing benzylamine (10 g) in CH_2Cl_2 was washed thrice with 10 mL portions of D_2O. The solution containing the deuterated product was dried over K_2CO_3, and the solvent was removed in vacuo. From the ^1H NMR spectrum, there was $> 90\%$ deuterium incorporation.

Reaction Procedures. The photocatalytic oxygenation of Ph_3P with O_2 was carried out by the following procedure. Typically, a chloroform solution (2 mL) containing Acr^+–Mes (4.12 mg, 1.0×10^{-5} mol) and Ph_3P (7.87 mg, 3.0×10^{-5} mol) in a Schlenk flask with a rubber septum was saturated with oxygen by bubbling oxygen through a stainless steel needle for 20 min. The solution was then irradiated with a 500 W xenon lamp (Ushio Optical ModelX SX-UID 500XAMQ) through a color filter glass (Asahi Techno Glass Y43) transmitting $\lambda > 430$ nm at 278 K. After 30 min photoirradiation, the corresponding $Ph_3P{=}O$ was identified by comparison of the GC retention time and the GC/MS spectrum (Shimadzu QP-5000) with those of an authentic sample.

The photocatalytic oxidation of benzylamine with O_2 was carried out as follows. Typically, an acetonitrile-d_3 solution (0.7 mL) containing Acr^+–Mes (1.44 mg, 3.5×10^{-6} mol) and benzylamine (4.87 mg, 3.8×10^{-5} mol) in a NMR tube with a rubber septum was saturated with oxygen by bubbling oxygen gas through a stainless steel needle for 20 min. The solution was then irradiated with a 500 W xenon lamp (Ushio Optical ModelX SX-UID 500XAMQ) through a color filter glass (Asahi Techno Glass Y43) transmitting $\lambda > 430$ nm at 278 K. After photoirradiation for 6 h, *N*-benzylidenebenzylamine was identified by comparing the ^1H NMR spectrum in comparison with that of an authentic sample. *N*-Benzylidenebenzylamine: ^1H NMR (300 MHz, CD_3CN) δ 4.77 (s, 2H), 7.22–7.32 (m, 1H), 7.33–7.38 (d, $J = 4.5$ Hz, 4H), 7.41–7.48 (m, 3H), 7.74–7.81 (m, 2H).

The amount of H_2O_2 was determined by titration by iodide ion as follows.[43–45] An O_2-saturated MeCN solution (3.0 mL) of Acr^+–Mes (1.0×10^{-4} mol dm^{-3}) and benzylamine (1.0×10^{-4} mol dm^{-3}) was photoirradiated for 2 h and the photoirradiated product mixture was treated with excess amount of NaI. The amount of I_3^- formed was then determined from the UV–vis spectrum ($\lambda_{max} = 361$ nm, $\varepsilon = 2.50 \times 10^4$ mol^{-1} dm^3 cm^{-1}).[44,45]

Quantum Yield Determinations. A standard actinometer [potassium trisoxalatoferrate(III)][46] was used to determine the quantum yield of the photocatalytic oxygenation of Ph_3P with O_2 in the presence Acr^+–Mes. Typically, a square quartz cuvette (10 mm i.d.), which contained a degassed MeCN or $CHCl_3$ solution (3.0 cm^3) of Acr^+–Mes (2.0×10^{-4} mol dm^{-3}) and Ph_3P (2.0×10^{-4} mol dm^{-3}), was irradiated with steady-state monochromatized light ($\lambda = 430$ nm) from a Shimadzu RF-5300PC fluorescence spectrophotometer. Under the conditions of actinometry experiments, the actinometer and Acr^+–Mes absorbed essentially all of incident light of $\lambda = 430$ nm. The light intensity of monochromatized light of $\lambda = 430$ nm was determined as 9.9×10^{-7} mol dm^{-3} s^{-1}. In addition, a square quartz cuvette (10 mm i.d.), which contained a degassed $CHCl_3$ solution (3.0 cm^3) of Acr^+–Mes (2.0×10^{-4} mol dm^{-3}) and Ph_3P (2.0×10^{-4} mol dm^{-3}), was irradiated with monochromatized laser flash ($\lambda = 430$ nm) from Nd:YAG laser (Continuum, SLII-10, 4–6 ns fwhm) at 430 nm. Under the conditions of actinometry experiments, the actinometer and Acr^+–Mes absorbed essentially all of incident light of $\lambda = 430$ nm. The light intensity of monochromatized light of $\lambda = 430$ nm was determined as 8.6×10^{-8} einstein/pulse. The photochemical reaction was monitored using a Hewlett Packard 8453 diode-array spectrophotometer. The quantum yields were determined from a decrease in absorbance due to Ph_3P ($\lambda = 302$ nm, $\varepsilon = 1.69 \times 10^3$ mol^{-1} dm^3 cm^{-1}) and benzylamine ($\lambda = 309$ nm, $\varepsilon = 2.7 \times 10^2$ mol^{-1} dm^3 cm^{-1}). In order to avoid the contribution by light absorption of the products, only the initial rates were used for determination of the quantum yields.

Fluorescence Quenching. Quenching experiments of the fluorescence of photocatalysts by Ph_3P or benzylamine were performed using a Shimadzu RF-5300PC fluorescence spectrophotometer. The monitoring wavelength was the maximum of the emission band for $AcrH^+$. The solutions were deoxygenated by argon purging for 10 min prior to the measurements. Relative emission intensities were measured for MeCN or $CHCl_3$ solutions containing $AcrH^+$ (5.0×10^{-6} mol dm^{-3}) with electron donors at various concentrations (0–8.0×10^{-2} mol dm^{-3}). There was no change in the shape, but there was a change in the intensity of the fluorescence spectrum by the addition of an electron donor. The Stern–Volmer relationship (Eq. 1) was obtained for

$$I_0/I = 1 + K_{SV}[D], \quad (1)$$

the ratio of the emission intensities in the absence and presence of electron donor (I_0/I) and concentrations of quenchers [D]. The fluorescence lifetimes (τ) are 37 ns for $AcrH^+$ and 31 ns in MeCN and $CHCl_3$, respectively.[47] The fluorescence lifetimes of $AcrH^+$ were measured by a Photon Technology International GL-3300 with a Photon Technology International GL-302, nitrogen laser/pumped dye laser system, equipped with a four channel digital delay/pulse generator (Stanford Research System Inc. DG535) and a motor driver (Photon Technology International MD-5020). Excitation wavelength was 430 nm using a toluene solution containing dimethyl-POPOP [1,4-bis(4-methyl-5-phenyl-2-oxazolyl)-

benzene] (Dojindo, Japan) as a laser dye. The observed quenching rate constants k_{obs} ($=K_{SV}\tau^{-1}$) were obtained from the Stern–Volmer constants K_{SV} and the emission lifetimes τ.

Electrochemical Measurements. Second harmonic ac voltammetry (SHACV)[48,49] measurements of Ph_3P, benzylamine, and *N*-benzylidenebenzylamine were performed with an ALS630B electrochemical analyzer in degassed acetonitrile containing 0.1 mol dm^{-3} $Bu_4N^+ClO_4^-$ (TBAP) as a supporting electrolyte or in chloroform containing 0.2 mol dm^{-3} TBAP at 298 K. The platinum working electrode (BAS, surface i.d. 1.6 mm) was polished with BAS polishing alumina suspension and rinsed with acetone before use. The counter electrode was a platinum wire (0.5 mm dia.). The measured potentials were recorded with respect to an $Ag/AgNO_3$ (0.01 mol dm^{-3}) reference electrode. The values of redox potentials (vs $Ag/AgNO_3$) were converted into those vs SCE by addition of 0.29 V.[50]

ESR Measurements. ESR measurements were performed on a JEOL X-band ESR spectrometer (JES-ME-LX) at 233 K. A quartz ESR tube (internal diameter: 1.5 mm) containing an argon-saturated di-*t*-butylperoxide solution of benzylamine (3.0×10^{-1} mol dm^{-3}) at 243 K was irradiated in the cavity of the ESR spectrometer with the focused light of a 1000-W high-pressure Hg lamp (Ushio-USH1005D) through an aqueous filter. The ESR spectra were measured under nonsaturating microwave power conditions. The amplitude of modulation was chosen to optimize the resolution and the signal-to-noise (S/N) ratio of the observed spectra.

Laser Flash Photolysis Measurements. Measurements of transient absorption spectra in the photochemical reactions of Acr^+–Mes with Ph_3P and benzylamine were performed according to the following procedure. A degassed CH_3CN_3 solution containing Acr^+–Mes (8.0×10^{-5} mol dm^{-3}) and benzylamine (1.3×10^{-2} mol dm^{-3}) was excited by Nd:YAG laser (Continuum, SLII-10, 4–6 ns fwhm) at 430 nm. Time courses of the transient absorption spectra were measured by using a continuous Xe-lamp (150 W) and an In GaAs-PIN photodiode (Hamamatsu 2949) as a probe light and a detector, respectively. The output from the photodiodes and a photomultiplier tube was recorded with a digitizing oscilloscope (Tektronix, TDS3032, 300 MHz). The transient spectra were recorded using fresh solutions in each laser excitation. The measurements of transient absorption spectra in the photochemical reaction of Bu^tOOBu^t with benzylamine were performed as follows. Typically, a degassed Bu^tOOBu^t solution containing benzylamine (3.0×10^{-1} mol dm^{-3}) was excited by Nd:YAG laser (Continuum, SLII-10, 4–6 ns fwhm) at 355 nm. All experiments were performed at 298 K.

Theoretical Calculations. Density-functional theory (DFT) calculations were performed on a COMPAQ DS20E computer. Geometry optimizations were carried out using the Becke3LYP functional and 6-31G* basis set[51] with unrestricted Hartree–Fock (UHF) formalism for benzylamine radical cation and $Ph_3P^{\bullet+}$ as implemented in the Gaussian 03 program. Graphical output of the computational results were generated with the Cerius^2 software program developed by Molecular Simulations Inc.

Results and Discussion

Photocatalytic Oxidation of Triphenylphosphine with O_2. Visible light irradiation ($\lambda > 430$ nm) of the absorption band of 9-mesityl-10-methylacridinium ion (Acr^+–Mes; 5.0×10^{-3} mol dm^{-3}) in an O_2-saturated chloroform ($CHCl_3$) solution containing triphenylphosphine (Ph_3P; 1.5×10^{-2} mol dm^{-3}) for 30 min by xenon lamp resulted in the formation of an oxygenated product, i.e., triphenylphosphine oxide ($Ph_3P{=}O$) in a 99% yield (Eq. 2).[52,53]

$$2\,Ph_3P + O_2 \xrightarrow{h\nu} 2\,Ph_3P{=}O \quad (2)$$

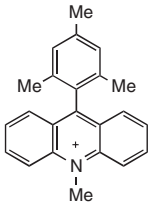

Acr^+–Mes

When Acr^+–Mes was replaced by 10-methylacridinium ion ($AcrH^+$), $Ph_3P{=}O$ was also obtained quantitatively after 60 min photoirradiation. It was confirmed that no photooxygenation of Ph_3P occurred without Acr^+–Mes or $AcrH^+$ under otherwise the same experimental conditions.

The quantum yields (Φ_P) of formation of $Ph_3P{=}O$ under photoirradiation with monochromatized light ($\lambda = 430$ nm) were determined from a decrease in absorbance due to Ph_3P using an actinometer (see Experimental). The dependence of Φ_P value on concentration of Ph_3P in the $AcrH^+$-catalyzed photooxygenation of Ph_3P with O_2 in air-saturated $CHCl_3$ is shown in Fig. 1a (closed square). The Φ_P value increases with increasing concentration of Ph_3P [Ph_3P] to reach a constant value. The saturated dependence of Φ_P on [Ph_3P] was converted to a linear plot of Φ_P^{-1} vs [Ph_3P]$^{-1}$ as shown in Fig. 1b. From the slope and intercept, the Φ_∞ and K_{obs} values were determined to be 0.57 and 2.1×10^2 mol^{-1} dm^3, respectively. The K_{obs} value is converted to rate constant (k_{obs}) using the relation: $k_{obs} = K_{obs}\tau^{-1}$ where τ is the lifetime of the singlet excited state of $AcrH^+$ ($^1AcrH^{+*}$: 31 ns) provided that $^1AcrH^{+*}$ reacts with Ph_3P in the photocatalytic reaction.[47] The k_{obs} value was determined to be 6.8×10^9 mol^{-1} dm^3 s^{-1}. The k_{obs} value was also obtained from the fluorescence quenching of $^1AcrH^{+*}$ by electron transfer from an electron donor (Ph_3P) to $^1AcrH^{+*}$ as 9.0×10^9 mol^{-1} dm^3 s^{-1} (See Supporting Information S1), which is comparable with the value (9.0×10^9 mol^{-1} dm^3 s^{-1}) obtained from the dependence of Φ_P on [Ph_3P] in Fig. 1a (closed square). This indicates that the $AcrH^+$-catalyzed photooxygenation of Ph_3P with O_2 proceeds via electron transfer from Ph_3P to $^1AcrH^{+*}$.

When $AcrH^+$ was replaced by Acr^+–Mes, the Φ_P values remained constant (0.58) irrespective of the concentration of Ph_3P as shown in Fig. 2 (closed circle), in contrast with the case of the $AcrH^+$-catalyzed photooxygenation of Ph_3P with O_2 (Fig. 1a). In the case of Acr^+–Mes, photoirradition of Acr^+–Mes results in formation of the electron-transfer state of Acr^+–Mes ($Acr^{\bullet}$–$Mes^{\bullet+}$).[36] Even small concentrations of Ph_3P can react with the $Mes^{\bullet+}$ moiety of $Acr^{\bullet}$–$Mes^{\bullet+}$ by electron transfer because the lifetime of $Acr^{\bullet}$–$Mes^{\bullet+}$ (ca. ms) is extremely long as compared to that of $^1AcrH^{+*}$ (31 ns).[36,47] This may be the reason why the Φ_P values are constant (0.58) in the concentration range of Ph_3P studied, Fig. 1a.

The dependence of Φ_P on the concentration of O_2 at a fixed concentration of Ph_3P (5.0×10^{-4} mol dm^{-3}) under photoirradiation with monochromatized light ($\lambda = 430$ nm) is shown in Fig. 2 (closed circle). The Φ_P value increases with increasing

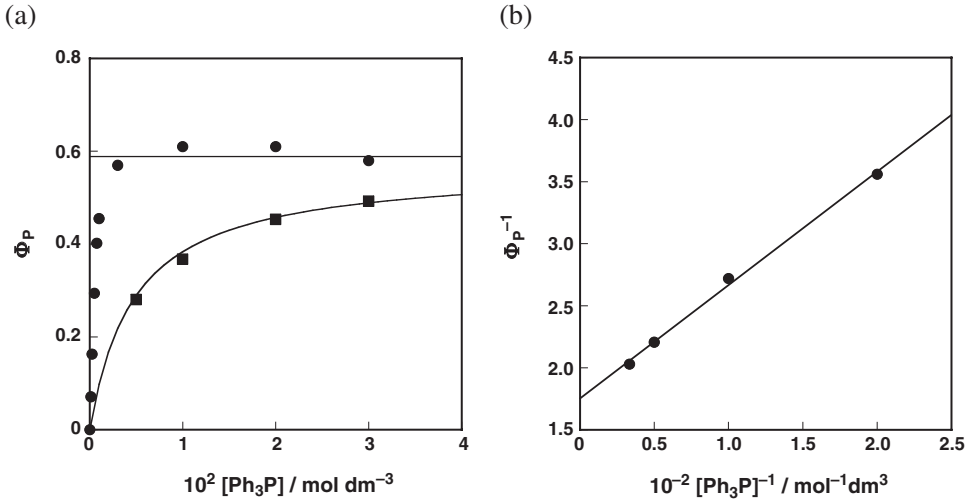

Fig. 1. (a) Dependence of quantum yield (Φ_P) of $Ph_3P{=}O$ on concentrations of Ph_3P for the photocatalytic oxygenation of Ph_3P with Acr^+–Mes (8.0×10^{-5} mol dm^{-3}, ●) and $AcrH^+$ (8.0×10^{-5} mol dm^{-3}, ■) in air-saturated $CHCl_3$. (b) Plot of $\Phi_P{}^{-1}$ on $[Ph_3P]^{-1}$ for the photocatalytic oxygenation of Ph_3P with $AcrH^+$ in air-saturated $CHCl_3$.

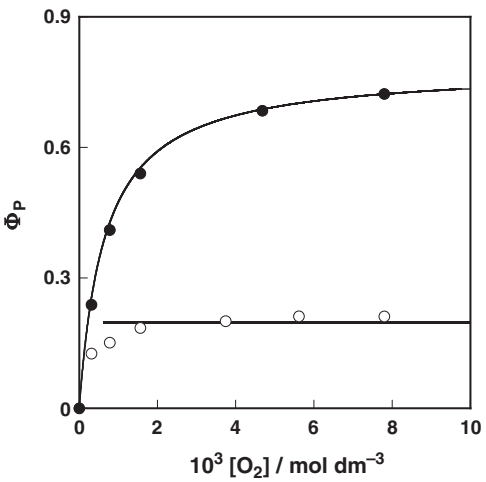

Fig. 2. Dependences of quantum yield (Φ_P) of $Ph_3P{=}O$ on concentration of O_2 for the photocatalytic oxygenation of Ph_3P (5.0×10^{-4} mol dm^{-3}) with Acr^+–Mes (8.0×10^{-5} mol dm^{-3}) photoirradiated by laser flash photolysis ($\lambda =$ 430 nm, 30 mJ/pulse) (○) and steady-state photolysis with monochromatized light ($\lambda = 430$ nm) (●).

concentration of O_2 to reaching a maximum at $\Phi_\infty = 0.78$. When the photoirradiation was carried out by using pulsed laser ($\lambda = 355$ nm, Nd-YAG laser, 10 Hz, 30 mJ/pulse) instead of steady-state photolysis with monochromatized light, however, the Φ_P values remained constant (0.21) irrespective of different the O_2 concentration. The origin of the different dependencies of Φ_P on concentration of O_2 between the laser excitation and steady-state photolysis with monochromatized light is discussed in the following section.

Photocatalytic Mechanisms of Oxygenation of Ph_3P. In order to elucidate the photocatalytic oxygenation mechanism, laser flash photolysis was used to detect the intermediates. Nanosecond laser excitation at 430 nm of a degassed anhydrous $CHCl_3$ solution of Acr^+–Mes resulted in the formation of the electron-transfer state ($Acr^{\bullet}$–$Mes^{\bullet+}$) via photoinduced electron transfer from the Mes moiety to the singlet excited state of the Acr^+ moiety.[36] The quantum yield for the formation of $Acr^{\bullet}$–$Mes^{\bullet+}$ has been previously determined to be nearly quantitative (98%).[36] Since the one-electron reduction potential of $Acr^{\bullet}$–$Mes^{\bullet+}$ ($E^0_{red} = 1.88$ V vs SCE) is more positive than the one-electron oxidation potential of Ph_3P ($E^0_{ox} =$ 1.20 V vs SCE), determined by second harmonic AC voltammetry (SHACV, See Experimental and Supporting Information Fig. S2), electron transfer from Ph_3P to the $Mes^{\bullet+}$ moiety in $Acr^{\bullet}$–$Mes^{\bullet+}$ is energetically feasible. Thus, the addition of Ph_3P to a $CHCl_3$ solution of Acr^+–Mes and laser photoexcitation afforded the Ph_3P radical cation ($Ph_3P^{\bullet+}$: $\lambda_{max} = 380$ nm)[54,55] as shown in Fig. 3a (open circles). The $Acr^{\bullet}$ moiety of $Acr^{\bullet}$–$Mes^{\bullet+}$ has an absorption band at 520 nm.[36] In the presence of Ph_3P, electron transfer from Ph_3P to the $Mes^{\bullet+}$ moiety occurs to produce $Ph_3P^{\bullet+}$ and $Acr^{\bullet}$–Mes, both of which have an absorption band at 520 nm. This is the reason why the absorption at 520 nm becomes larger in the presence of Ph_3P (open circles in Fig. 3a) as compared with that in the absence of Ph_3P (closed circles in Fig. 3b). The formation and decay of the absorption at 380 nm are the same as those at 520 nm. It is important to note that the absorption band due to the $Acr^{\bullet}$ moiety remains virtually the same in the absence of O_2 (Fig. 3b). This indicates clearly that $Ph_3P^{\bullet+}$ is formed by electron transfer from Ph_3P to $Acr^{\bullet}$–$Mes^{\bullet+}$ rather than by direct photoinduced electron transfer from Ph_3P to the singlet excited state of the Acr^+ moiety in Acr^+–Mes.

The rate of formation of $Ph_3P^{\bullet+}$ increases with increasing concentration of Ph_3P as shown in Fig. 4a. The formation rate obeys pseudo-first-order kinetics, and the pseudo-first-order rate constant increases linearly with increasing concentration of Ph_3P (Fig. 4b). The second-order rate constant of electron transfer from Ph_3P to $Acr^{\bullet}$–$Mes^{\bullet+}$ was determined from the slope of the linear plot in Fig. 4b to be 9.2×10^9 mol^{-1} dm^3 s^{-1}, which is close to be the diffusion-limited value as expected for the exergonic electron transfer.[56]

The observed residual absorption at 380 nm is attributed

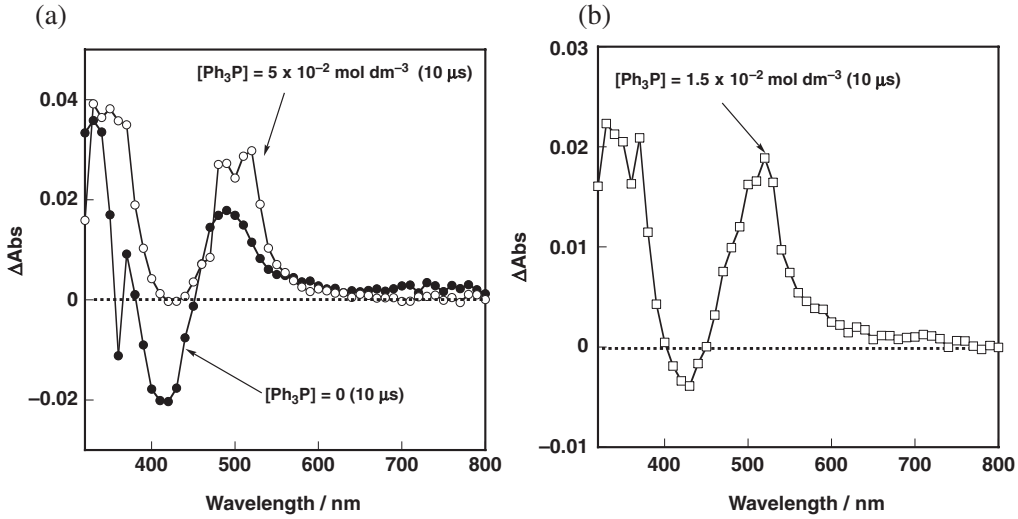

Fig. 3. Transient absorption spectra observed in photoinduced electron-transfer oxidation of Ph_3P with Acr^+–Mes (8.0×10^{-5} mol dm^{-3}) taken 10 μs after laser excitation at 430 nm (a) in deaerated $CHCl_3$ at 298 K. (b) in O_2-saturated $CHCl_3$ at 298 K.

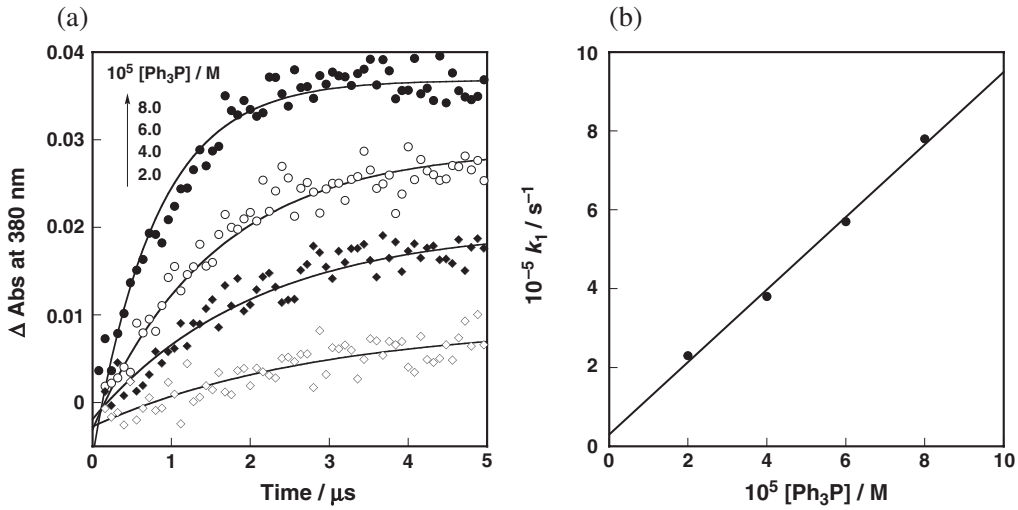

Fig. 4. (a) Time profiles at 380 nm of transient absorption due to the formation of $Ph_3P^{\bullet+}$ observed by photoexcitation of a deaerated MeCN solution containing Acr^+–Mes (8.0×10^{-5} mol dm^{-3}) and various concentrations of Ph_3P (2.0×10^{-5}–8.0×10^{-5} mol dm^{-3}) with single-exponential curve. (b) Plot of pseudo-first-order rate constant (k_1) vs concentration of Ph_3P.

to $Ph_3P^{\bullet+}$ ($\varepsilon = 3600$ mol^{-1} dm^3 cm^{-1})[54] which slowly decays, Fig. 5. The decay obeys the second-order kinetics as shown in the inset of Fig. 5. From the slope of the second-order plot, the decay rate constant was determined to be 1.1×10^{10} mol^{-1} dm^3 s^{-1}, which is close to diffusion rate in $CHCl_3$. This process corresponds to the back electron transfer from $O_2^{\bullet-}$ to $Ph_3P^{\bullet+}$ and radical coupling to give the oxygenated adduct.

The photocatalytic mechanism involving the radical intermediates detected in Fig. 4 is shown in Scheme 1. Photoexcitation of Acr^+–Mes gives the long-lived electron-transfer state ($Acr^{\bullet}$–$Mes^{\bullet+}$). The $Acr^{\bullet}$ and $Mes^{\bullet+}$ moieties can reduce and oxidize O_2 and $Ph_3P^{\bullet+}$, respectively, to give superoxide anion ($O_2^{\bullet-}$) and $Ph_3P^{\bullet+}$, respectively. Radical coupling between $Ph_3P^{\bullet+}$ and $O_2^{\bullet-}$ may afford the dioxygen adduct (Ph_3PO_2) (reaction pathway A in Scheme 1), which may be a cyclic peroxide as reported in the literature.[57] The final oxygenated product ($Ph_3P{=}O$) is known to be formed by the reaction of Ph_3PO_2 with Ph_3P in competition with the dissociation to Ph_3P and O_2 (Scheme 1).[54,57–59] Ph_3PO_2 may also be formed via addition of O_2 to $Ph_3P^{\bullet+}$ to give $Ph_3PO_2^{\bullet+}$ and back electron transfer from $Acr^{\bullet}$–Mes to $Ph_3PO_2^{\bullet+}$ (reaction pathway B in Scheme 1).[58,59]

Based on Scheme 1, the competition between the pathways A and B is determined by the rate of the reaction of $Ph_3P^{\bullet+}$ with O_2 and $O_2^{\bullet-}$. The rate constant of the reaction of $Ph_3P^{\bullet+}$ with O_2 (k_B) was reported to be 7.3×10^6 mol^{-1} dm^3 s^{-1},[58] and the first-order rate constant (k_1) of the reaction of $Ph_3P^{\bullet+}$ with O_2 in O_2-saturated $CHCl_3$ ($[O_2] = 7.8 \times 10^{-3}$ mol^{-1} dm^3)[60] was estimated to be 5.7×10^4 s^{-1}. On the other hand, the rate constant of the reaction of $Ph_3P^{\bullet+}$ with $O_2^{\bullet-}$ (k_A) was determined to be 1.1×10^{10} mol^{-1} dm^3 s^{-1} (Fig. 5). The concentration of $Ph_3P^{\bullet+}$ formed in electron transfer from Ph_3P to $Acr^{\bullet}$–$Mes^{\bullet+}$ should be the same as concentration of $O_2^{\bullet-}$ formed in electron transfer from $Acr^{\bullet}$–Mes to O_2 (Scheme 1).

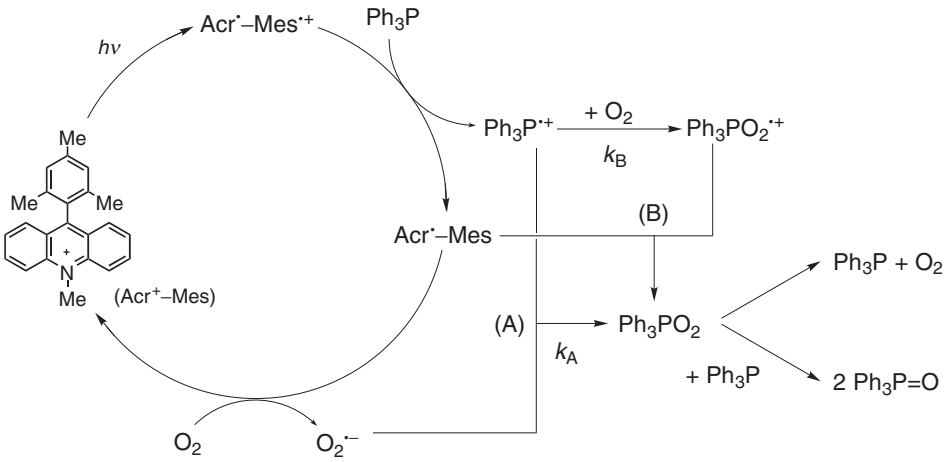

Scheme 1.

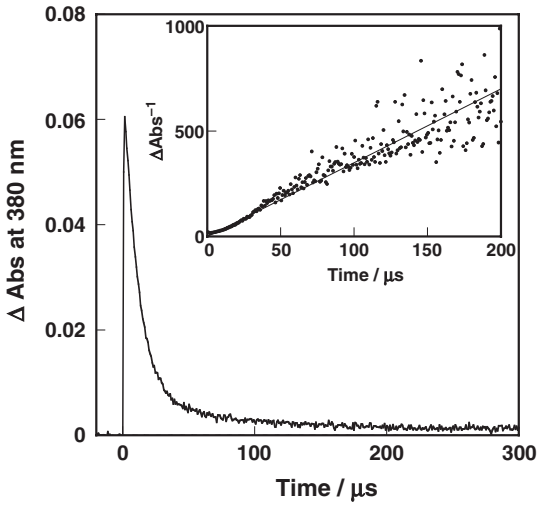

Fig. 5. Decay time profile at 380 nm of transient absorption due to $Ph_3P^{\bullet+}$ observed by photoexcitation of an oxygen-saturated MeCN solution containing Acr^+–Mes (8.0×10^{-5} mol dm^{-3}). Inset: second-order plot.

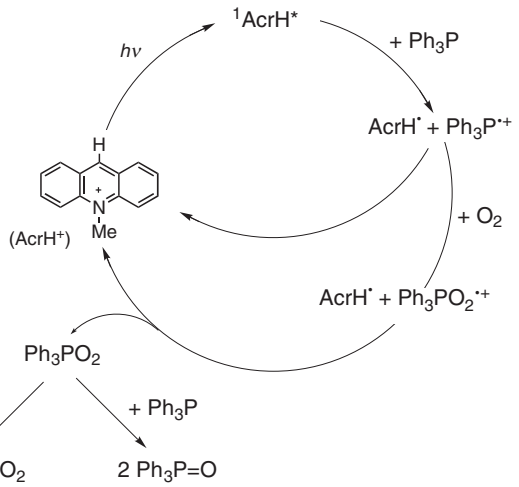

Scheme 2.

The concentration of $Ph_3P^{\bullet+}$ in the laser flash photolysis was determined to be 5.1×10^{-6} mol dm^{-3} from the transient absorption of $Acr^{\bullet}$–$Mes^{\bullet+}$ ($\lambda_{max} = 500$ nm and $\varepsilon_{500} = 3.5 \times 10^3$ mol^{-1} dm^3 cm^{-1})[36] in Fig. 4. In this case, the k_1 value of the reaction of $Ph_3P^{\bullet+}$ with $O_2^{\bullet-}$ (5.1×10^{-6} mol dm^{-3}) was determined to be 5.6×10^4 s^{-1}. Thus, the ratio of pathway A to B was estimated to be 1:1 from the ratio of the k_1 values (5.6×10^4 to 5.7×10^4). This indicates that the photooxygenation proceeds via pathway A as well as pathway B in the case of laser pulse excitation.

In the case of the steady-state photoirradiation with monochromatized light ($\lambda = 430$ nm), the concentration of $Ph_3P^{\bullet+}$ and $O_2^{\bullet-}$ is given by Eq. 4, where In is the light intensity ($In = 9.9 \times 10^{-7}$ mol dm^{-3} s^{-1}) and $k_A = 1.1 \times 10^{10}$ mol^{-1} dm^3 s^{-1}, by applying a steady-state approximation to $Ph_3P^{\bullet+}$ and $O_2^{\bullet-}$ in Scheme 1. The concentration of $O_2^{\bullet-}$ was estimated to be 9.1×10^{-9} mol dm^{-3} by using Eq. 3,

$$[O_2^{\bullet-}] = [Ph_3P^{\bullet+}] = (In/k_A)^{1/2}, \quad (3)$$

assuming that the quantum yield for the radical coupling of $Ph_3P^{\bullet+}$ and $O_2^{\bullet-}$ is almost unity. The first-order rate constant (k_1) of the reaction of $Ph_3P^{\bullet+}$ with $O_2^{\bullet-}$ (9.1×10^{-9} mol dm^{-3}) was to be 1.0×10^2 s^{-1}. Thus, the ratio of pathway A to B under the steady-state photoirradiation with monochromatized light ($\lambda = 430$ nm) is approximately 1:570 from the ratio of the k_1 values (6.0×10^3 to 1.0×10^2). Ph_3PO_2 reacts with the large excess of Ph_3P to give Ph_3P=O via O–O bond cleavage.[57]

In contrast to the case of Acr^+–Mes in Scheme 1, the $AcrH^+$-catalyzed photooxygenation of Ph_3P with O_2 proceeds via electron transfer from Ph_3P to $^1AcrH^{+*}$ (vide supra) as shown in Scheme 2.[61] Photoinduced electron transfer from Ph_3P to $^1AcrH^{+*}$ is energetically feasible, because the E^0_{ox} value of Ph_3P (1.20 V vs SCE) is lower than the E^0_{red} value of $^1AcrH^{+*}$ (2.32 V).[47] $Ph_3P^{\bullet+}$, produced by the electron transfer from Ph_3P to $^1AcrH^{+*}$, reacts with O_2 to yield triphenylphosphine peroxide radical cation ($Ph_3PO_2^{\bullet+}$). Then, electron transfer from $AcrH^{\bullet}$ to $Ph_3PO_2^{\bullet+}$ occurs to yield $AcrH^+$ and Ph_3PO_2.[57] Ph_3PO_2 reacts with Ph_3P to yield Ph_3P=O via O–O bond cleavage in competition with the dissociation to Ph_3P and O_2 (Scheme 2) as the case of the photocatalytic oxygenation of Ph_3P with O_2 catalyzed by Acr^+–Mes in Scheme 1. The quantum yields of the $AcrH^+$-catalyzed pho-

tooxygenation are always lower compared to that of Acr^+–Mes (Fig. 1a), This is ascribed to the absence of the radical coupling reaction between $Ph_3P^{\bullet+}$ and $O_2^{\bullet-}$ (Scheme 2). In the case of $AcrH^+$, no $O_2^{\bullet-}$ is formed, because the electron-transfer reduction of O_2 by $AcrH^\bullet$ (-0.43 V vs SCE)[47] is energetically impossible. Thus, Acr^+–Mes is a better photocatalyst than $AcrH^+$.

Photocatalytic Oxidation of Benzylamine. Visible light irradiation of the absorption band ($\lambda > 430$ nm) of Acr^+–Mes (5.0×10^{-3} mol dm^{-3}) in an O_2-saturated acetonitrile (MeCN) solution containing benzylamine (6.0×10^{-2} mol dm^{-3}) resulted in the formation of *N*-benzylidenebenzylamine, $PhCH_2N{=}CHPh$ (Eq. 4).

$$2PhCH_2NH_2 + O_2 \xrightarrow[Acr^+\text{–Mes}]{h\nu} PhCH_2N{=}CHPh + H_2O_2 + NH_3. \quad (4)$$

The yield of $PhCH_2N{=}CHPh$ and H_2O_2 was determined to be 58 and 46% by ^{1}H NMR and iodometry, respectively (see Experimental).[62,63]

Laser flash photolysis was used to elucidate the mechanistic details for photocatalytic oxidation. Transient absorption spectra taken after the nanosecond laser excitation at 430 nm of a degassed MeCN solution of Acr^+–Mes in the absence and presence of benzylamine are shown in Fig. 6. The absorption band due to the $Mes^{\bullet+}$ moiety ($\lambda_{max} = 470$ nm)[36] of $Acr^\bullet$–$Mes^{\bullet+}$ was quenched by the addition of benzylamine. However, no transient absorption due to benzylamine radical cation was observed by nanosecond laser flash photolysis, probably because of the rapid decay of benzylamine radical cation (vide infra).[64] The bimolecular rate constant of electron transfer from benzylamine to $Acr^\bullet$–$Mes^{\bullet+}$ (k_{et}) was determined from the decays of transient absorption due to the $Mes^{\bullet+}$ moiety in the presence of various concentrations of benzylamine as shown in Fig. 7. The decay at 470 nm obeys pseudo-first-order kinetics and the pseudo-first-order rate constant increases linearly with increasing concentration of benzylamine (Fig. 7b). The k_{et} value was determined from the slope of Fig. 7b to be 3.3×10^9 mol^{-1} dm^3 s^{-1}. The one-electron oxidation potential (E^0_{ox}) of benzylamine was determined by SHACV to be 0.62 V vs SCE (see Supporting Information Fig. S3a). Electron transfer from benzylamine to $Acr^\bullet$–$Mes^{\bullet+}$ is energetically feasible, because the E^0_{red} value of benzylamine is more negative than that of $Acr^\bullet$–$Mes^{\bullet+}$ ($E^0_{red} = 1.88$ V vs SCE). On the other hand, $O_2^{\bullet-}$ is formed by electron transfer from the $Acr^\bullet$ moiety to O_2.[39] Consequently, proton transfer from benzylamine radical cation to $O_2^{\bullet-}$ occurs to yield $HO_2^\bullet$ and the neutral radical species.

Whether the neutral species derived from deprotonation of benzylamine radical cation is a nitrogen-centered radical ($PhCH_2NH^\bullet$) or a benzyl type radical ($PhCH^\bullet NH_2$) has yet to be determined (Scheme 3). The radical species has been directly detected by ESR in the hydrogen abstraction from benzylamine by *t*-butoxyl radical in order to determine the structure of the hydrogen-abstracted radical (Scheme 4).[65–67]

The photoirradiation of a degassed neat solution of

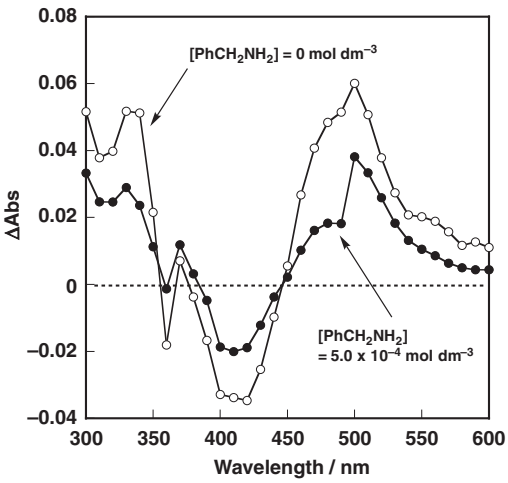

Fig. 6. Transient absorption spectra observed in photoinduced electron-transfer oxidation of benzylamine (5.0×10^{-4} mol dm^{-3}) with Acr^+–Mes (8.0×10^{-5} mol dm^{-3}) taken 10 μs after laser excitation at 430 nm in deaerated CH_3CN at 298 K.

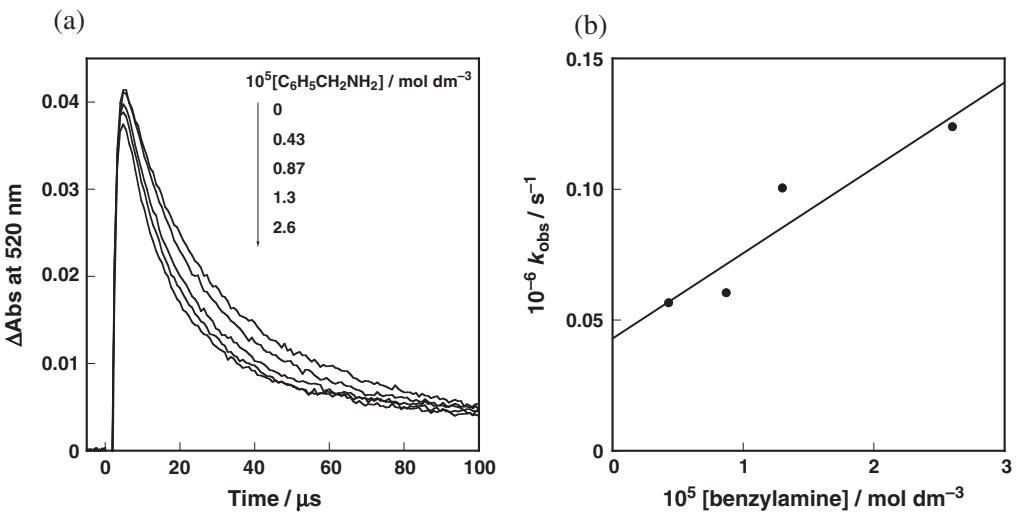

Fig. 7. (a) Decay time profiles at 520 nm in the photooxidation of benzylamine in MeCN containing Acr^+–Mes (8.0×10^{-5} mol dm^{-3}). (b) Plot of pseudo-first-order rate constant vs concentration of benzylamine.

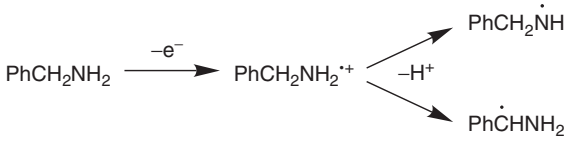

Scheme 3.

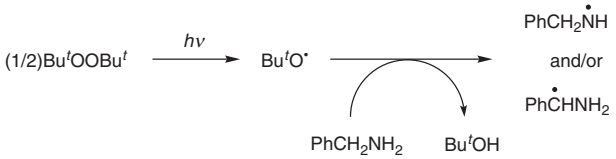

Scheme 4.

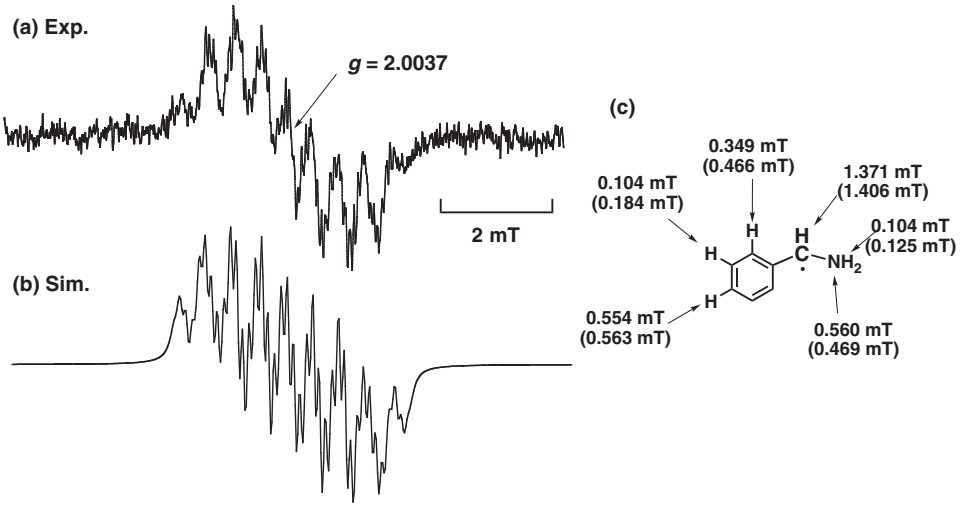

Fig. 8. (a) ESR spectrum under irradiation of a deaerated Bu^tOOBu^t solution containing benzylamine (3.0×10^{-1} mol dm^{-3}) at 243 K. (b) The computer simulated spectrum. (c) Hyperfine coupling constants (the values in parentheses are those determined by DFT calculation).

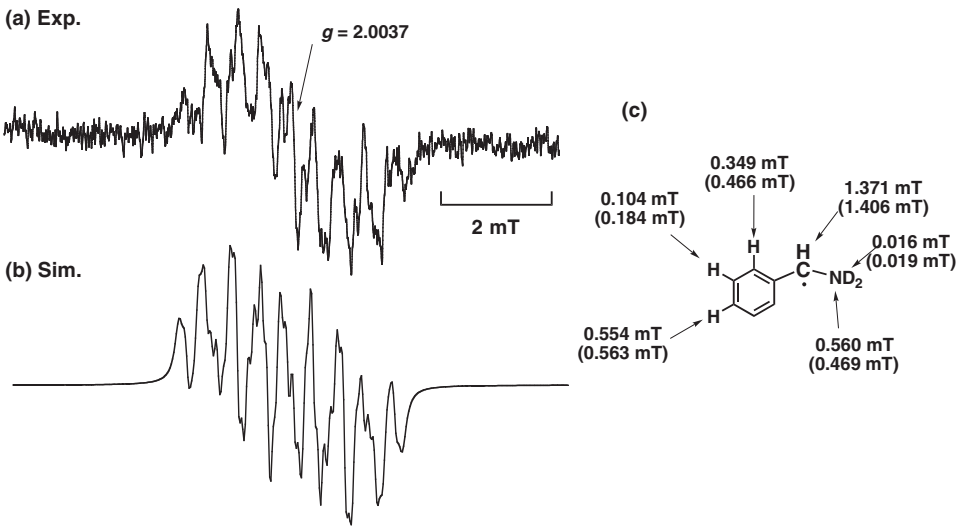

Fig. 9. (a) ESR spectrum under irradiation of a deaerated Bu^tOOBu^t solution containing [*N*,*N*-$^2H_2$]benzylamine (3.0×10^{-1} mol dm^{-3}) at 243 K. (b) The computer simulated spectrum. (c) Hyperfine coupling constants (the values in parentheses are those determined by DFT calculation).

Bu^tOOBu^t containing benzylamine (3.0×10^{-1} mol dm^{-3}) at 243 K with a 1000 W high-pressure mercury lamp resulted in formation of a hydrogen-abstracted radical, which was clearly observed by ESR as shown in Fig. 8. The hydrogen-abstracted radical is formed via hydrogen abstraction from benzylamine by *t*-butoxyl radical ($Bu^tO^\bullet$), which is generated by the homolytic cleavage of the O–O bond of Bu^tOOBu^t.[65–67] The *g* value (2.0037) of the ESR signal in Fig. 8 is typical for that of a benzyl radical. From the well-resolved ESR spectrum in Fig. 8a, the hyperfine coupling constants (*hfc*) were determined, Fig. 8c. The computer simulated spectrum using these *hfc* values (Fig. 8b) agrees with the observed ESR spectrum. Deuterium substitution of the two hydrogen atoms of the amino group of benzylamine ([*N*,*N*-$^2H_2$] benzylamine) confirmed the *hfc* assignment in Fig. 9 since the observed ESR spectrum agrees with the computer simulated spectrum using the same *hfc* values except for the value of the deuterium ($I = 1$) at the N-position. The *hfc* values of the hydrogen-abstracted radi-

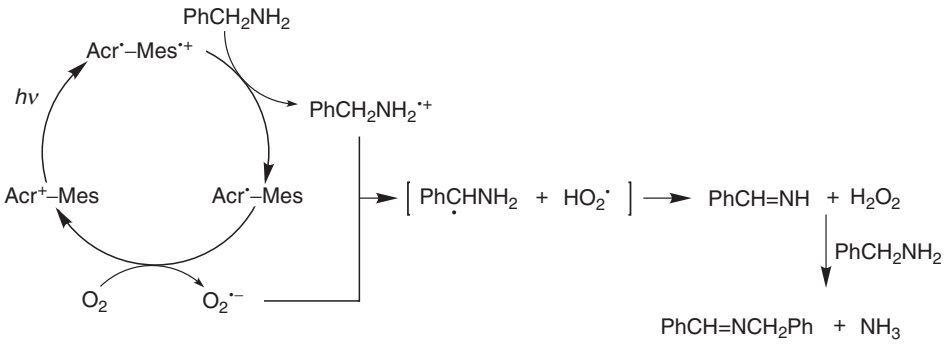

Scheme 5.

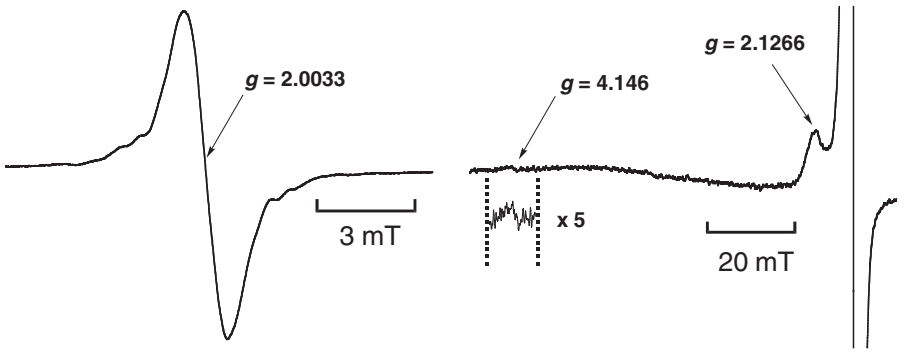

Fig. 10. ESR spectra under photoirradiation of an O_2-saturated benzylamine solution containing Acr^+–Mes (5.0×10^{-3} mol dm^{-3}) at 123 K.

cal of [*N*,*N*-$^2H_2$] benzylamine become smaller by the magnetogyric ratio of proton to deuterium (0.153) as compared to those of non-deuterated benzylamine.[68]

The *hfc* assignment is also supported by the DFT calculation (see the calculated *hfc* values in parentheses in Fig. 9b). Total energy of both hydrogen-abstracted radicals were also determined by DFT using the UB3LYP/6-31G* basis set (see Experimental). The energy of the benzyl radical is 8 kcal mol^{-1} lower than that of nitrogen-centered radical. This indicates that that deprotonation of benzylamine radical cation occurs at the α-position.

Based on the above results, the reaction mechanism of photocatalytic oxidation of benzylamine Acr^+–Mes with molecular oxygen is shown in Scheme 5. Photoirradiation of Acr^+–Mes gives the electron-transfer state, which can act as an oxidant for benzylamine and a reductant for molecular oxygen, resulting in the formation of a benzylamine radical cation and superoxide anion ($O_2^{\bullet-}$). Then, proton transfer from benzylamine radical cation to superoxide anion ($O_2^{\bullet-}$) occurs to give the α-hydrogen-abstracted benzylamine radical and hydroperoxyl radical ($HO_2^{\bullet}$). The benzylamine radical reacts with $HO_2^{\bullet}$ to yield benzylideneamine (PhCH=NH) and hydrogen peroxide (H_2O_2). No further oxygenation of $PhCH_2N$=CHPh occurs because the E^0_{ox} value of $PhCH_2N$=CHPh (2.09 V vs SCE: see Supporting Information Fig. S3b) is more positive than the E^0_{red} value of $Acr^{\bullet}$–$Mes^{\bullet+}$. Instead, PhCH=NH reacts with benzylamine to produce the final product, $PhCH_2N$=CHPh (Scheme 5).[63,69]

Detection of Radical Intermediates by ESR. The occurrence of photoinduced electron transfer in the photocatalytic oxygenation reactions described above has also been confirmed by ESR measurements. When an O_2-saturated benzylamine solution of Acr^+–Mes was irradiated at 123 K, a triplet ESR signal was observed as shown in Fig. 10. A small signal was also observed at $g = 4.0$ due to the $\Delta M_S = 2$ transition. The "$\Delta M_S = 2$" line in the region of $g = 4.0$ is a diagnostic marker for the triplet state.[70–73] The zero-field splitting parameters D and E ($\cong$0) were determined from the triplet signals due to the radical ion pair ($PhCH_2NH_2^{\bullet+}$ and $O_2^{\bullet-}$) and the values are listed in Table 1. When $PhCH_2NH_2$ was replaced by Ph_3P, the ESR signal of the triplet contact radical ion pair between $Ph_3P^{\bullet+}$ and $O_2^{\bullet-}$ was observed, and therefore, the value of D and E were larger (Fig. 11). Since D depends on the distance between two electrons with parallel spins, the average distance of two spins can be evaluated from the values of D, and the distances between the radical ions (r) are also listed in Table 1.

Table 1. Zero-Field Splitting Parameters (D, E), and Distance of Contact Ion Pair (r)

	D/mT	E/mT	r/Å
Triphenylphosphine	7.0	0.69	7.4
Benzylamine	4.4	0.37	8.6

The r value of the radical ion pair of $PhCH_2NH_2^{\bullet+}$ and $O_2^{\bullet-}$ (8.6 Å) is smaller than that of $Ph_3P^{\bullet+}$ and $O_2^{\bullet-}$ (7.4 Å). The optimized structures of $Ph_3P^{\bullet+}$ and $PhCH_2NH_2^{\bullet+}$ were calculated by density-functional theory (DFT) using the UB3LYP functional and 6-31G* basis set (See Experimental), and are shown in Fig. 12. The spin distributions of radical cations are also shown in Fig. 12. The unpaired electrons of $Ph_3P^{\bullet+}$ are localized on the P atom. In contrast, the unpaired

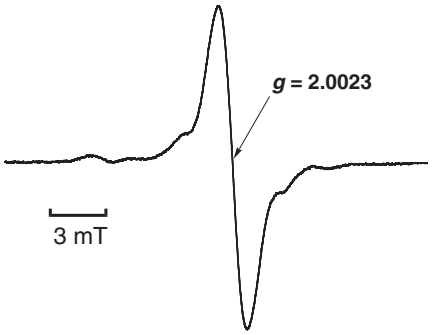

Fig. 11. ESR spectrum under photoirradiation of an O_2-saturated CH_3CN solution containing Ph_3P (1.0×10^{-2} mol dm^{-3}) and Acr^+–Mes (5.0×10^{-3} mol dm^{-3}) at 123 K.

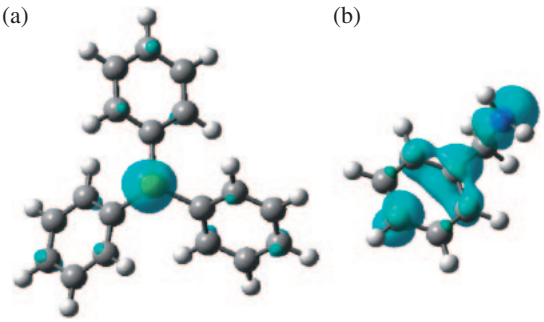

Fig. 12. Optimized structures and spin distributions of (a) $Ph_3P^{\bullet+}$ and (b) benzylamine radical cation obtained from DFT calculations at the UB3LYP/6-31G* basis set.

electrons of $PhCH_2NH_2^{\bullet+}$ are delocalized on nitrogen atom and aromatic carbons. Thus, $O_2^{\bullet-}$ interacts more strongly with $Ph_3P^{\bullet+}$ than with to that of $PhCH_2NH_2^{\bullet+}$. This may result in the shorter distance of the $Ph_3P^{\bullet+}$–$O_2^{\bullet-}$ pair as compared with the $PhCH_2NH_2^{\bullet+}$–$O_2^{\bullet-}$ pair.

In conclusion, Acr^+–Mes has been shown to act as an efficient photocatalyst for the oxygenation of different types of substrates via the reaction of substrate radical cations and superoxide anion. Radical intermediates in the photocatalytic oxidation of substrates with O_2 were successfully detected by laser flash photolysis and ESR measurements to clarify the photocatalytic mechanisms.

This work was partially supported by a Grant-in-Aid (Nos. 16205020 and 17750039) from the Ministry of Education, Culture, Sports, Science and Technology, Japan.

Supporting Information

Fluorescence quenching of $^1AcrH^{+*}$ by Ph_3P (S1) and electrochemical measurements (S2 and S3). This material is available free of charge on the web at http://www.csj.jp/journals/bcsj/.

References

1 J. Fossey, D. Lefort, J. Sorba, *Free Radicals in Organic Chemistry*, Wiley, New York, **1995**.

2 B. Giese, *Radicals in Organic Synthesis: Formation of Carbon–Carbon Bonds*, ed. by J. E. Baldwin, Pergamon Press, Oxford, **1986**.

3 a) *Radicals in Organic Synthesis*, ed. by P. Renaoud, M. P. Sibi, Wiley-VCH, Weinheim, **2001**, Vol. 2. b) H. Togo, *Advanced Free Radical Reactions for Organic Synthesis*, Elsevier, Amsterdam, **2004**.

4 *Free Radicals in Biology and Environment*, ed. by F. Minisci, Kluwer, Dordrecht, **1997**.

5 M. Schmittel, M. K. Ghorai, *Electron Transfer in Chemistry*, ed. by V. Balzani, Wiley-VCH, Weinheim, **2001**, Vol. 2, pp. 5–54.

6 L. Eberson, *Electron Transfer Reactions in Organic Chemistry: Reactivity and Structure*, Springer, Heidelberg, **1987**, Vol. 25.

7 S. Fukuzumi, *Advances in Electron Transfer Chemistry*, ed. by P. S. Mariano, JAI Press, Greenwich, **1992**, Vol. 2, p. 65.

8 S. Fukuzumi, *Electron Transfer in Chemistry*, ed. by V. Balzani, Wiley-VCH, Weinheim, **2001**, Vol. 4, pp. 3–67.

9 S. Das, V. Suresh, *Electron Transfer in Chemistry*, ed. by V. Balzani, Wiley-VCH, Weinheim, **2001**, Vol. 2, pp. 379–456.

10 C. Amatore, A. R. Brown, *J. Am. Chem. Soc.* **1996**, *118*, 1482.

11 a) S. Fukuzumi, K. Ohkubo, T. Okamoto, *J. Am. Chem. Soc.* **2002**, *124*, 14147. b) S. Fukuzumi, Y. Fujii, T. Suenobu, *J. Am. Chem. Soc.* **2001**, *123*, 10191.

12 *Photoinduced Electron Transfer*, ed. by M. A. Fox, M. Chanon, Elsevier, Amsterdam, **1988**.

13 a) F. Müller, J. Mattay, *Chem. Rev.* **1993**, *93*, 99. b) M. Mella, M. Fagnoni, M. Freccero, E. Fasani, A. Albini, *Chem. Soc. Rev.* **1998**, *27*, 81.

14 a) M. Julliard, M. Chanon, *Chem. Rev.* **1983**, *83*, 425. b) F. D. Lewis, *Acc. Chem. Res.* **1986**, *19*, 401. c) U. C. Yoon, P. S. Mariano, *Acc. Chem. Res.* **1992**, *25*, 233.

15 G. J. Kavarnos, N. J. Turro, *Chem. Rev.* **1986**, *86*, 401.

16 E. R. Gaillard, D. G. Whitten, *Acc. Chem. Res.* **1996**, *29*, 292.

17 S. Fukuzumi, H. Imahori, *Photochemistry of Organic Molecules in Isotropic and Anisotropic Media*, ed. by V. Ramamurthy, K. S. Schanze, Marcel Dekker, New York, **2003**, pp. 227–273.

18 S. M. Hubig, J. K. Kochi, *Electron Transfer in Chemistry*, ed. by V. Balzani, Wiley-VCH, Weinheim, **2001**, Vol. 2, pp. 618–676.

19 a) J. K. Kochi, *Angew. Chem., Int. Ed. Engl.* **1988**, *27*, 1227. b) R. Rathore, J. K. Kochi, *Adv. Phys. Org. Chem.* **2000**, *35*, 193.

20 S. Fukuzumi, K. Mochida, J. K. Kochi, *J. Am. Chem. Soc.* **1979**, *101*, 5961.

21 G. J. Kavarnos, N. J. Turro, *Chem. Rev.* **1986**, *86*, 401.

22 D. G. Whitten, C. Chesta, X. Ci, M. A. Kellett, V. W. W. Yam, In *Photochemical Processes in Organized Molecular Systems*, ed. by K. Honda, Elsevier, Amsterdam, **1991**.

23 G. Pandey, In *Topics in Current Chemistry: Photoinduced Electron Transfer V*, Springer-Verlag, Berlin, **1993**, Vol. 168, pp. 175–221.

24 a) D. Mangion, D. R. Arnold, *Acc. Chem. Res.* **2002**, *35*, 297. b) T. Miyashi, H. Ikeda, Y. Takahashi, *Acc. Chem. Res.* **1999**, *32*, 815.

25 a) U. C. Yoon, P. S. Mariano, R. S. Givens, B. W. Atwater, In *Advances in Electron Transfer Chemistry*, ed. by P. S. Mariano, P. S. JAI Press, Greenwich, CT, **1994**, Vol. 4, pp. 117–205. b) H. D. Roth, In *Topics in Current Chemistry: Photoinduced Electron Transfer IV*, ed. by J. Mattay, Springer-Verlag, Berlin, **1992**, Vol. 163, pp. 131–245. c) F. D. Saeva, In *Advances in Electron Transfer Chemistry*, ed. by P. S. Mariano, JAI Press,

Greenwich, CT, **1994**, Vol. 4, pp. 1–25.

26 a) S. Fukuzumi, In *Advances in Electron Transfer Chemistry*, ed. by P. S. Mariano, JAI Press, Greenwich, CT, **1992**, Vol. 2, pp. 67–175. b) S. Fukuzumi, S. Itoh, In *Advances in Photochemistry*, ed. by D. C. Neckers, D. H. Volman, John Wiley & Sons, New York, **1999**, Vol. 25, p. 107. c) A. Sancar, In *Advances in Electron Transfer Chemistry*, ed. by P. S. Mariano, JAI Press, Greenwich, CT, **1992**, Vol. 2, pp. 215–272.

27 J. Lind, X. Shen, G. Merényi, B. Ö. Jonsson, *J. Am. Chem. Soc.* **1989**, *111*, 7654.

28 a) M. S. McDowell, J. H. Espenson, A. Bakac, *Inorg. Chem.* **1984**, *23*, 2232. b) K. Zahir, J. H. Espenson, A. Bakac, *J. Am. Chem. Soc.* **1988**, *110*, 5059.

29 L. Eberson, R. Gonzales-Luque, J. Lorentzon, M. Merchan, B. O. Roos, *J. Am. Chem. Soc.* **1993**, *115*, 2898.

30 E. G. German, A. M. Kuznetsov, I. Efremenko, M. Sheintuch, *J. Phys. Chem. A* **1999**, *103*, 10699.

31 S. Fukuzumi, S. Fujita, Y. Suenobu, H. Yamada, H. Imahori, Y. Araki, O. Ito, *J. Phys. Chem. A* **2002**, *106*, 1241.

32 a) C. S. Foote, *Acc. Chem. Res.* **1968**, *1*, 104. b) C. S. Foote, E. L. Clennan, *Properties and Reactions of Singlet Oxygen*, In *Active Oxygen in Chemistry*, ed. by C. S. Foote, J. S. Valentine, A. Greenberg, J. F. Liebman, Chapman and Hall, New York, **1995**, pp. 105–140.

33 a) D. R. Kearns, *Chem. Rev.* **1971**, *71*, 395. b) L. M. Stephenson, M. J. Grdina, M. Orfanopoulos, *Acc. Chem. Res.* **1980**, *13*, 419.

34 a) *Singlet Oxygen Reactions with Organic Compounds and Polymers*, ed. by B. Ranby, J. F. Rabeck, Wiley, New York, **1978**. b) *Singlet Oxygen*, ed. by A. A. Frimer, CRC Press, Boca Raton, FL, **1985**, Vols. I–IV. c) A. Griesbeck, In *CRC Handbook of Organic Photochemistry and Photobiology*, ed. by W. M. Horspool, P.-S. Song, CRC Press, Boca Raton, FL, **1995**, p. 301.

35 M. A. Iesce, *Synthetic Organic Photochemistry*, ed. by A. G. Greisbeck, J. Mattay, Marcel Dekker, New York, **2005**, pp. 299–363.

36 S. Fukuzumi, H. Kotani, K. Ohkubo, S. Ogo, N. V. Tkachenko, H. Lemmetyinen, *J. Am. Chem. Soc.* **2004**, *126*, 1600.

37 K. Ohkubo, H. Kotani, S. Fukuzumi, *Chem. Commun.* **2005**, 4520.

38 H. Kotani, K. Ohkubo, S. Fukuzumi, *J. Am. Chem. Soc.* **2004**, *126*, 15999.

39 K. Ohkubo, T. Nanjo, S. Fukuzumi, *Org. Lett.* **2005**, *7*, 4265.

40 Tetrahydrofuran as a solvent of the Grignard reaction is better than dichloromethane reported previously.[38]

41 S. Fukuzumi, S. Koumitsu, K. Hironaka, T. Tanaka, *J. Am. Chem. Soc.* **1987**, *109*, 305.

42 K. J. Smith, E. D. Bergbreiter, M. Newcomb, *J. Org. Chem.* **1985**, *50*, 4549.

43 R. D. Mair, A. J. Graupner, *Anal. Chem.* **1964**, *36*, 194.

44 S. Fukuzumi, S. Kuroda, T. Tanaka, *J. Am. Chem. Soc.* **1985**, *107*, 3020.

45 S. Fukuzumi, M. Ishikawa, T. Tanaka, *J. Chem. Soc., Perkin Trans. 2* **1989**, 1037.

46 C. G. Hatchard, C. A. Parker, *Proc. R. Soc. London, Ser. A* **1956**, *235*, 518.

47 K. Ohkubo, K. Suga, K. Morikawa, S. Fukuzumi, *J. Am. Chem. Soc.* **2003**, *125*, 12850.

48 A. J. Bard, L. R. Faulkner, *Electrochemical Methods: Fundamentals and Applications*, John Wiley & Sons, New York, **2001**, Chap. 10, pp. 368–416.

49 The SHACV method provides a superior approach to directly evaluating the one-electron redox potentials in the presence of a follow-up chemical and reaction, relative to the better-known dc and fundamental harmonic ac methods. See: a) M. R. Wasielewski, R. Breslow, *J. Am. Chem. Soc.* **1976**, *98*, 4222. b) E. M. Arnett, K. Amarnath, N. G. Harvey, J. Cheng, *J. Am. Chem. Soc.* **1990**, *112*, 344.

50 C. K. Mann, K. K. Barnes, In *Electrochemical Reactions in Non-aqueous Systems*, Mercel Dekker, New York, **1970**.

51 a) A. D. Becke, *J. Chem. Phys.* **1993**, *98*, 5648. b) C. Lee, W. Yang, R. G. Parr, *Phys. Rev. B* **1988**, *37*, 785. c) W. J. Hehre, L. Radom, P. V. R. Schleyer, J. A. Pople, In *Ab Initio Molecular Orbital Theory*, Wiley, New York, **1986**.

52 A trace amount of $Ph_2P(=O)OPh$ (e.g., 0.6%) was formed in the reaction of Ph_3P with singlet oxygen.[53] In the photocatalytic oxygenation of Ph_3P with Acr^+–Mes, no $Ph_2P(=O)OPh$ was detected.

53 S. Tsuji, M. Kondo, K. Ishiguro, Y. Sawaki, *J. Org. Chem.* **1993**, *58*, 5055.

54 M. Nakamura, M. Miki, T. Majima, *J. Chem. Soc., Perkin Trans. 2* **2000**, 1447.

55 The formation of $Ph_3P^{\bullet+}$ was monitored at 380 nm in order to avoid the decay of the absorption due to the $Acr^{\bullet}$ moiety at the shorter wavelengths.

56 G. J. Kavarnos, *Fundamentals of Photoinduced Electron Transfer*, Wiley-VCH, New York, **1993**.

57 D. G. Ho, R. Gao, J. Celaje, H.-Y. Chung, M. Selke, *Science* **2003**, *302*, 259.

58 Z. B. Alfassil, P. Neta, B. Beaver, *J. Phys. Chem. A* **1997**, *101*, 2153.

59 S. Yasui, S. Tojo, T. Majima, *J. Org. Chem.* **2005**, *70*, 1276.

60 R. Battio, H. L. Clever, C. L. Young, *IUPAC Solubility Data Series*, Pergamon Press, Oxford, **1981**, Vol. 7.

61 The $AcrH^+$-catalyzed photooxygenation of substrates have already been studied extensively.[47] See: a) K. Suga, K. Ohkubo, S. Fukuzumi, *J. Phys. Chem. A* **2003**, *107*, 4339. b) K. Suga, K. Ohkubo, S. Fukuzumi, *J. Phys. Chem. A* **2005**, *109*, 10168. c) K. Suga, K. Ohkubo, S. Fukuzumi, *J. Phys. Chem. A* **2006**, *110*, 3860. d) K. Ohkubo, K. Suga, S. Fukuzumi, *Chem. Commun.* **2006**, 2018.

62 No formation of $PhCH_2N{=}CHPh$ was observed in $AcrH^+$-catalyzed photooxidation since the photocatalyst was decomposed by the formation of a large amount of the adducts.

63 F. D. Lewis, T.-I. Ho, *J. Am. Chem. Soc.* **1977**, *99*, 7991.

64 a) C. G. Shaefer, K. S. Peter, *J. Am. Chem. Soc.* **1980**, *102*, 7567. b) F. D. Lewis, *Acc. Chem. Res.* **1986**, *19*, 401.

65 P. J. Krusic, J. K. Kochi, *J. Am. Chem. Soc.* **1968**, *90*, 7155.

66 a) J. K. Kochi, P. J. Krusic, D. R. Eaton, *J. Am. Chem. Soc.* **1969**, *91*, 1877. b) P. J. Krusic, J. K. Kochi, *J. Am. Chem. Soc.* **1969**, *91*, 3938. c) P. J. Krusic, J. K. Kochi, *J. Am. Chem. Soc.* **1969**, *91*, 3942. d) J. K. Kochi, P. J. Krusic, *J. Am. Chem. Soc.* **1969**, *91*, 3944. e) J. A. Howard, E. Furimsky, *Can. J. Chem.* **1974**, *52*, 555.

67 a) S. Fukuzumi, K. Shimoosako, T. Suenobu, Y. Watanabe, *J. Am. Chem. Soc.* **2003**, *125*, 9074. b) H. Kitaguchi, K. Ohkubo, S. Ogo, S. Fukuzumi, *J. Am. Chem. Soc.* **2005**, *127*, 6605. c) K. Ohkubo, Y. Moro-oka, S. Fukuzumi, *Org. Biomol. Chem.* **2006**, *4*, 999.

68 ESR measurements of the hydrogen-abstracted radical of benzylamine in Figs. 8 and 9 were carried out under same experimental and instrumental conditions i.e., concentration,

temperature, and modulation width.

69 a) S. Naya, H. Ohtoshi, M. Nitta, *J. Org. Chem.* **2006**, *71*, 176. b) S. Naya, J. Nishimura, M. Nitta, *J. Org. Chem.* **2005**, *70*, 9780.

70 F. D. Lewis, T.-I. Ho, J. T. Sinpson, *J. Am. Chem. Soc.* **1982**, *104*, 1924.

71 J. E. Wertz, J. R. Bolton, In *Electron Spin Resonance, Elementary Theory and Practical Applications*, McGraw-Hill, New York, **1972**.

72 S. Fukuzumi, T. Okamoto, K. Ohkubo, *J. Phys. Chem. A* **2003**, *107*, 5412.

73 T. Da Ros, M. Prato, D. M. Guldi, M. Ruzzi, L. Pasimeni, *Chem. Eur. J.* **2001**, *7*, 816.